

Sideband Instabilities and Defects of Quasipatterns

Blas Echebarria¹ and Hermann Riecke²

Department of Engineering Sciences and Applied Mathematics, Northwestern University, 2145 Sheridan Rd, Evanston, IL, 60208, USA

Abstract

Quasipatterns have been found in dissipative systems ranging from Faraday waves in vertically vibrated fluid layers to nonlinear optics. We describe the dynamics of octagonal, decagonal and dodecagonal quasipatterns by means of coupled Ginzburg-Landau equations and study their stability to sideband perturbations analytically using long-wave equations as well as by direct numerical simulation. Of particular interest is the influence of the phason modes, which are associated with the quasiperiodicity, on the stability of the patterns. In the dodecagonal case, in contrast to the octagonal and the decagonal case, the phase modes and the phason modes decouple and there are parameter regimes in which the quasipattern first becomes unstable with respect to phason modes rather than phase modes. We also discuss the different types of defects that can arise in each kind of quasipattern as well as their dynamics and interactions. Particularly interesting is the decagonal quasipattern, which allows two different types of defects. Their mutual interaction can be extremely weak even at small distances.

1 Introduction

Since the discovery of quasicrystals in 1984 [1], much attention has been paid to the properties of these materials. In contrast to perfect crystals they lack periodicity, but preserve long-range orientational order. Due to this lack of periodicity quasicrystals may have non-crystallographic rotational symmetry

¹ Corresponding author. Tel.: (617) 373-2924, Fax.: (617) 373-2943, e-mail: blas@presto.physics.neu.edu. Current address: Physics Department, Northeastern University, Boston, MA 02115.

² E-mail: h-riecke@northwestern.edu

and, in fact, materials have been found with five, eight, ten or twelve-fold rotational axes.

In dissipative systems the possibility of quasiperiodic structures, or quasipatterns, was also suggested some time ago [2]. Since then they have been observed in Faraday waves with one- and two-frequency forcing [3,4] and in nonlinear optics [5]. Marangoni convection with a deformable interface has also been suggested to support quasipatterns [6], although they have not been observed so far.

In Faraday waves a great variety of patterns has been observed. They include superlattices, rhombic states, oscillons, as well as quasipatterns [7–9]. In order for superlattices and quasipatterns to be stable the mutual suppression of plane-wave modes of different orientation has to be sufficiently weak. This can be due to a few, somewhat different mechanisms. When forced with two frequencies, the system can exhibit simultaneously instabilities at two different wavelengths and the quasipatterns and superlattices appear near this bicritical point. The angle between the wavevectors of the destabilizing modes depends on the ratio of the two wavelengths. It determines whether the resulting patterns corresponds to a superlattice or a quasipattern. A mechanism involving two length scales was suggested some time ago for quasicrystals [10] and studied in dissipative systems by means of a modified Swift-Hohenberg equation with two marginal modes [11]. The second length scale need not be associated with a proper instability. It can be sufficient that one of the modes is weakly damped. The interaction of the unstable mode with this damped mode can then lead to a reduction in the mutual suppression of modes subtending a certain angle [12]. Alternatively, the interaction with the damped mode can strongly enhance the saturating self-coupling term which then effectively leads to a reduction of the competition over a wide range of angles [13,14]. This favors patterns with a large number of modes. Calculations of the coefficients of the amplitude equations for Faraday waves suggest that this is indeed the case [15,16].

In nonlinear optics the optical field in a nonlinear cavity can be rotated in order to obtain a structure with the desired number of modes [5]. In these systems it is also possible to arrange patterns with two different spatial scales, leading to complex quasicrystalline structures [17–19].

The relative stability of perfect quasipatterns has already been addressed [2]. In the present paper we are interested in the stability of n -fold quasipatterns to sideband perturbations, in particular to slowly varying modulations. We will assume that the physical fields can be expanded as a sum of Fourier modes rotated by $2\pi/n$ relative to each other (similar to the density wave picture of quasicrystals), with slowly varying amplitudes in space and time. Using symmetry arguments we determine a set of coupled Ginzburg-Landau equa-

tions for these amplitudes. Due to the lack of periodicity, a rigorous derivation from the basic equations using a center manifold reduction has not been possible so far. However, we will consider the Ginzburg-Landau equations as phenomenological models and aim to extract conclusions that can be verified experimentally.

As is well known in the study of quasicrystals, the long-wave dynamics of the system is governed by two types of modes: phonons and phasons. The former ones are marginal modes arising from spatial translation symmetries. The phasons, on the other hand, are additional marginal modes characteristic of quasicrystals and appear because of the quasiperiodic nature of these structures. As we will see later, in octagonal and dodecagonal quasipatterns they have a very simple geometrical interpretation, since these quasipatterns can be viewed as two superimposed square (hexagonal) lattices rotated by $2\pi/8$ ($2\pi/12$). The phason modes correspond to *relative* translations between the two lattices. It is worth mentioning that when the angle between the two lattices satisfies certain conditions, the whole structure becomes periodic with a wavelength larger than that of the individual lattices: this is known as a superlattice [20]. In this case, extra resonance conditions among the modes are satisfied [21], and the phason modes become damped and can, in principle, be eliminated in a long-wave analysis.

The paper is organized as follows. In the next three sections we study octagonal, decagonal and dodecagonal quasipatterns arising from steady bifurcations. In each case we start with the amplitude equations and study various simple solutions and their relative stability. Our main focus is the long-wave dynamics of the quasiperiodic solutions. We derive coupled equations for the phonon- and phason-type modes, obtaining the diffusive counterpart to the elastic equations for a quasicrystal [22]. We then calculate the long-wave stability limits for sideband perturbations and investigate numerically the behavior arising from the instabilities. In section 5 we discuss the different types of defects that appear in each kind of quasipattern and their dynamics and interactions. Conclusions are presented in section 6.

2 Octagonal Quasipatterns

2.1 Ginzburg-Landau Equations

We consider a quasipattern composed of four modes, $\psi = \eta \sum_{n=1}^4 A_n(\mathbf{x}, t) e^{i\mathbf{k}_n \cdot \hat{\mathbf{x}}} + c.c. + h.o.t$, where $\eta \ll 1$ and the amplitudes $A_i(\mathbf{x}, t)$ satisfy the equations (af-

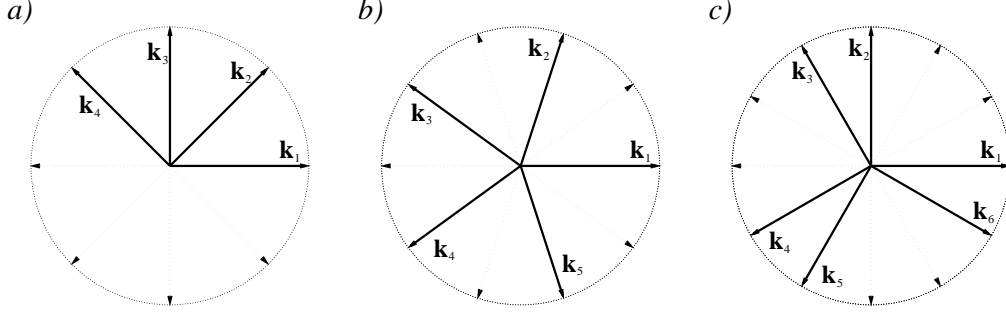


Fig. 1. Fourier modes composing the a) octagonal, b) decagonal and c) dodecagonal quasipatterns. Solid vectors denote the modes described by Eqs. (1), (39), and (85, 86), respectively.

ter rescaling):

$$\partial_t A_i = \mu A_i + (\hat{\mathbf{n}}_i \cdot \tilde{\nabla})^2 A_i - A_i \left[|A_i|^2 + \nu |A_{i+2}|^2 + \gamma (|A_{i+1}|^2 + |A_{i+3}|^2) \right], \quad (1)$$

with μ the control parameter and $\hat{\mathbf{n}}_i$ the unit vector in the direction of the wavenumber \mathbf{k}_i (see Fig. 1a). The amplitudes A_i depend on slow scales $x = \eta \hat{x}$ and $t = \eta^2 \hat{t}$. Here and in the following the indices are repeated cyclicly with period 4. Thus, A_5 corresponds to A_1 , etc. The coefficients ν and γ measure the interaction between modes that subtend an angle of $\pi/2$ and $\pi/4$, respectively.

Eqs. (1) have gradient structure

$$\partial_t A_i = -\frac{\partial \mathcal{F}}{\partial A_i}, \quad (2)$$

and can be derived from the Lyapunov functional

$$\begin{aligned} \mathcal{F} \equiv \int \int dx dy F = \int \int dx dy \sum_{i=1}^4 \left[-\mu |A_i|^2 + |(\hat{\mathbf{n}}_i \cdot \tilde{\nabla})^2 A_i|^2 + \frac{1}{2} |A_i|^4 \right. \\ \left. + \gamma |A_i|^2 |A_{i+1}|^2 + \frac{\nu}{2} |A_i|^2 |A_{i+2}|^2 \right]. \end{aligned} \quad (3)$$

Therefore, the dynamics of the system are relaxational.

In order to calculate the different solutions we write $A_j = a_j e^{i\phi_j}$, with a_j real. Splitting into real and imaginary parts yields

$$\partial_t a_i = \mu a_i - a_i [a_i^2 + \nu a_{i+2}^2 + \gamma (a_{i+1}^2 + a_{i+3}^2)], \quad (4)$$

$$\partial_t \phi_i = 0. \quad (5)$$

The amplitudes can be considered to be real ($\phi_1 = \dots = \phi_4 = 0$). There are five different kinds of simple solutions [2] (see Fig. 2):

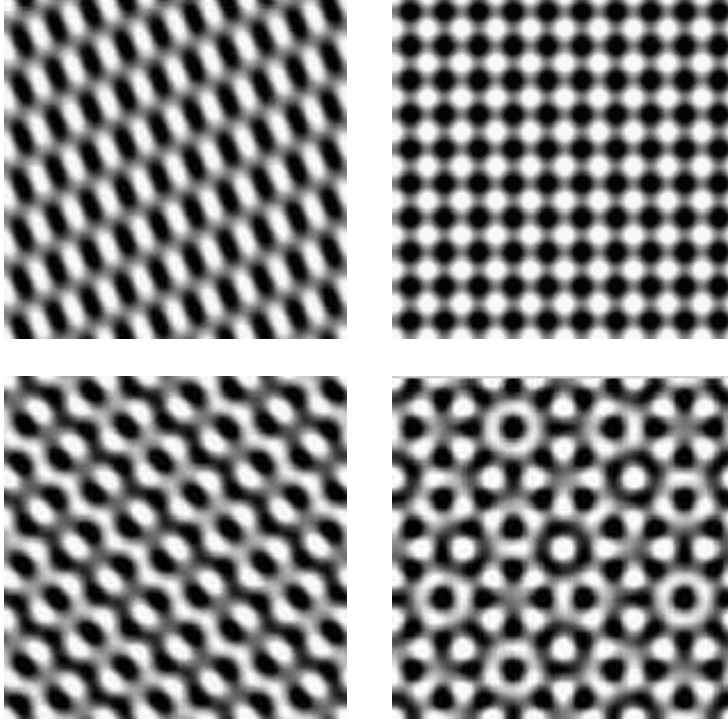


Fig. 2. Octagonal case. Different types of solutions of Eqs. (1), obtained by reconstructing the physical field ψ from the amplitudes A_i . a) Rectangles, b) squares, c) 1D quasipattern and d) octagonal quasipattern.

- (1) Rolls: $a_2 = a_3 = a_4 = 0$ and $a_1 = \sqrt{\mu}$. The value of the Lyapunov functional for rolls is: $F_{Roll} = -\mu^2/2$.
- (2) Squares: $a_2 = a_4 = 0$ and $a_1 = a_3 = \sqrt{\mu/(\nu + 1)}$, $F_{Sq} = -\mu^2/(\nu + 1)$.
- (3) Rectangles: $a_3 = a_4 = 0$ and $a_1 = a_2 = \sqrt{\mu/(\gamma + 1)}$, $F_{Rect} = -\mu^2/(\gamma + 1)$.
- (4) One-dimensional quasipattern: $a_4 = 0$ and

$$a_2 = \sqrt{\frac{\mu(1 + \nu - 2\gamma)}{1 + \nu - 2\gamma^2}}, \quad a_1 = a_3 = \sqrt{\frac{\mu(1 - \gamma)}{1 + \nu - 2\gamma^2}}. \quad (6)$$

$$\Rightarrow F_{1DQ} = -\frac{\mu^2}{2} \frac{3 + \nu - 4\gamma}{1 + \nu - 2\gamma^2}. \quad (7)$$

It is quasiperiodic in the direction of \mathbf{k}_2 and periodic along \mathbf{k}_4 . As is typical for solutions with submaximal isotropy, this solution exists only over a limited range of the nonlinear coefficients, $(1 + \nu - 2\gamma)(1 - \gamma) > 0$. It is always unstable [2].

(5) Quasipattern: $a_1 = \dots = a_4 = R$, with R satisfying,

$$R = \sqrt{\frac{\mu}{1 + \nu + 2\gamma}} \Rightarrow F_Q = -\frac{2\mu^2}{1 + \nu + 2\gamma}. \quad (8)$$

The conditions for linear stability of these solutions are given by

- (1) Rolls: $\nu > 1, \gamma > 1$.
- (2) Squares: $\gamma > (1 + \nu)/2, -1 < \nu < 1$.
- (3) Rectangles: $\nu > 1, -1 < \gamma < 1$.
- (4) Quasipattern: $-(1 + \nu)/2 < \gamma < (1 + \nu)/2, -1 < \nu < 1$.

2.2 Longwave analysis

We assume that the conditions for the two-dimensional quasipattern to be stable with respect to homogeneous perturbations are satisfied and study its stability to sideband perturbations. In particular, we study the stability of the pattern as a function of its wavenumber. A perfect quasipattern with wavenumber \mathbf{k} slightly different from critical is given by $A_i = Re^{iq\hat{\mathbf{n}}_i \cdot \mathbf{x}}$, with $R = |A_1| = |A_2| = |A_3| = |A_4| = \sqrt{(\mu - q^2)/(1 + \nu + 2\gamma)}$ and $\eta q = |\mathbf{k} - \mathbf{k}_c|$. We expand around this solution, $A_i = (R + r_i)e^{i(q\hat{\mathbf{n}}_i \cdot \mathbf{x} + \phi_i)}$. Considering first only homogeneous perturbations ($r_i = r_i(t), \phi_i = \phi_i(t)$) and separating real and imaginary parts, the linearized equations for the perturbations are:

$$\partial_t r_i = -2R^2 r_i - 2\nu R^2 r_{i+2} - 2\gamma R^2 (r_{i+1} + r_{i+3}), \quad (9)$$

$$\partial_t \phi_i = 0. \quad (10)$$

For the amplitude perturbations there are three eigenvalues, two corresponding to one-dimensional eigenspaces, $\sigma_{\hat{r}_1} = -2R^2(1 + \nu + 2\gamma)$, for $v_{\hat{r}_1} = [r_1 = 1, r_2 = 1, r_3 = 1, r_4 = 1]/2$, and $\sigma_{\hat{r}_2} = -2R^2(1 + \nu - 2\gamma)$ for $v_{\hat{r}_2} = [-1, 1, -1, 1]/2$. The other eigenvalue $\sigma_{\hat{r}_3, \hat{r}_4} = -2R^2(1 - \nu)$ corresponds to a two dimensional eigenspace spanned by $v_{\hat{r}_3} = [-1, -1, 1, 1]/2, v_{\hat{r}_4} = [-1, 1, 1, -1]/2$.

The four phases are marginal modes. Physically it is more convenient to rearrange them into phonon and phason modes. The first two are related to translations in space and can be written as

$$u_{\phi_x}^T = [\phi_1 = 1, \phi_2 = \cos(2\pi/8), \phi_3 = \cos(4\pi/8), \phi_4 = \cos(6\pi/8)], \quad (11)$$

$$u_{\phi_y}^T = [0, \sin(2\pi/8), \sin(4\pi/8), \sin(6\pi/8)]. \quad (12)$$

There still remains a two-dimensional subspace orthogonal to this one. An orthonormal basis for it is given by

$$u_{\varphi_1}^T = [1, -\cos(2\pi/8), \cos(4\pi/8), -\cos(6\pi/8)], \quad (13)$$

$$u_{\varphi_2}^T = [0, -\sin(2\pi/8), \sin(4\pi/8), -\sin(6\pi/8)]. \quad (14)$$

This choice of the phason modes corresponds to relative translations (in the x- and y-directions, respectively) between the two square lattices that compose the quasipattern. It is worth mentioning that the phason modes do not transform as a vector. In fact, under rotations by an angle θ the transformation of the phason field $\tilde{\varphi} = (\varphi_1, \varphi_2)$ corresponds to that of a regular vector for a rotation by an angle 5θ (cf. (30.31)).

When spatial modulations are included the perturbation equations become

$$\begin{aligned} \partial_t r_i = & -2qR(\hat{\mathbf{n}}_i \cdot \tilde{\nabla})\phi_i + (\hat{\mathbf{n}}_i \cdot \tilde{\nabla})^2 r_i \\ & -2R^2 r_i - 2\nu R^2 r_{i+2} - 2\gamma R^2 (r_{i+1} + r_{i+3}), \end{aligned} \quad (15)$$

$$\partial_t \phi_i = (\hat{\mathbf{n}}_i \cdot \tilde{\nabla})^2 \phi_i + \frac{2q}{R} (\hat{\mathbf{n}}_i \cdot \tilde{\nabla}) r_i. \quad (16)$$

Now the phase modes are no longer marginal, but exhibit diffusive dynamics. In order to study these long-wave dynamics we define a small parameter ϵ and introduce slow time and space scales: $T = \epsilon t$, $\mathbf{X} = \epsilon^{1/2} \mathbf{x}$. The amplitude and phase perturbations are expanded as:

$$r_i(\mathbf{X}, T) = \epsilon \sum_{j=1}^4 \hat{r}_j^i(\mathbf{X}, T) v_{\hat{r}_j}^i \quad (17)$$

$$\begin{aligned} \phi_i(\mathbf{X}, T) = & \epsilon^{1/2} [\phi_x(\mathbf{X}, T) u_{\phi_x}^i + \phi_y(\mathbf{X}, T) u_{\phi_y}^i, \\ & + \varphi_1(\mathbf{X}, T) u_{\varphi_1}^i + \varphi_2(\mathbf{X}, T) u_{\varphi_2}^i]. \end{aligned} \quad (18)$$

Inserting the expansion into Eqs. (15), (16), we obtain at order $\epsilon^{1/2}$ the eigenvalues for the homogeneous perturbations, at order ϵ a relation between the stable and marginal modes of the type $\hat{r}_i = f_i(\nabla\phi_x, \nabla\phi_y, \nabla\varphi_1, \nabla\varphi_2)$, and at order $\epsilon^{3/2}$ a solvability condition for the marginal modes. This gives us the slow, longwave dynamics. In component form the final equations are:

$$\begin{aligned} \partial_T \phi_x = & D_1 \nabla^2 \phi_x + (D_2 - D_1) \partial_X (\nabla \cdot \vec{\phi}) \\ & + D_3 (\partial_X^2 \varphi_1 - 2\partial_{XY}^2 \varphi_2 - \partial_Y^2 \varphi_1), \end{aligned} \quad (19)$$

$$\begin{aligned} \partial_t \phi_y = & D_1 \nabla^2 \phi_y + (D_2 - D_1) \partial_Y (\nabla \cdot \vec{\phi}) \\ & + D_3 (-\partial_X^2 \varphi_2 - 2\partial_{XY}^2 \varphi_1 + \partial_Y^2 \varphi_2), \end{aligned} \quad (20)$$

$$\begin{aligned} \partial_t \varphi_1 = \frac{1}{2} & \left[(D_4 + D_5) \nabla^2 \varphi_1 + (D_4 - D_5) (\partial_X^2 \varphi_2 - \partial_Y^2 \varphi_2 - 2\partial_{XY}^2 \varphi_1) \right] \quad (21) \\ & + D_3 (\partial_X^2 \phi_x - 2\partial_{XY}^2 \phi_y - \partial_Y^2 \phi_x), \end{aligned}$$

$$\begin{aligned} \partial_t \varphi_2 = \frac{1}{2} & \left[(D_4 + D_5) \nabla^2 \varphi_2 + (D_4 - D_5) (\partial_X^2 \varphi_1 - \partial_Y^2 \varphi_1 + 2\partial_{XY}^2 \varphi_2) \right] \quad (22) \\ & + D_3 (-\partial_X^2 \phi_y - 2\partial_{XY}^2 \phi_x + \partial_Y^2 \phi_y), \end{aligned}$$

where the values of the coefficients are given by

$$D_1 = \frac{1}{4} - \frac{q^2}{u}, \quad (23)$$

$$D_2 = \frac{3}{4} - \frac{q^2}{u} - \frac{2q^2}{v_1} = D_1 + D'_2, \quad (24)$$

$$D_3 = D_1, \quad (25)$$

$$D_4 = D_1, \quad (26)$$

$$D_5 = \frac{3}{4} - \frac{q^2}{u} - \frac{2q^2}{v_2} = D_1 + D'_5, \quad (27)$$

with $v_1 = 2R^2(1 + \nu + 2\gamma)$, $v_2 = 2R^2(1 + \nu - 2\gamma)$, $u = 2R^2(1 - \nu)$, and R given by Eq. (8) with μ replaced by $\mu - q^2$. Eqs. (19)-(22) are the diffusive analogue of the elastic equations for octagonal quasicrystals, and their form can be deduced directly by means of symmetry arguments.

A more compact notation, in which the symmetries become more evident, can be achieved by writing the phonon and phason modes as complex fields. Let $\phi = \phi_x + i\phi_y$, $\varphi = \varphi_1 + i\varphi_2$ and $\nabla = \partial_X + i\partial_Y$. Then the former expressions become:

$$\partial_t \phi = D_1 |\nabla|^2 \phi + (D_2 - D_1) \nabla (\bar{\nabla} \phi + \nabla \bar{\phi}) + D_3 e^{i\alpha} \bar{\nabla}^2 \bar{\phi}, \quad (28)$$

$$\partial_t \varphi = \frac{1}{2} (D_4 + D_5) |\nabla|^2 \varphi + \frac{i}{2} (D_4 - D_5) \nabla^2 \bar{\varphi} + D_3 e^{i\alpha} \bar{\nabla}^2 \bar{\varphi} \quad (29)$$

The angle α depends on the basis that is chosen for the phonon and phason modes. Since the specific choice does not have any physical relevance, α does not appear in the dispersion relation. In our case, $\alpha = 0$. Now it is easy to see that these equations are invariant under rotations of $n\pi/4$. In fact, under such a rotation $\phi \rightarrow e^{n\pi i/4} \phi$, $\nabla \rightarrow e^{n\pi i/4} \nabla$, $\varphi \rightarrow e^{5n\pi i/4} \varphi$, and consequently

$$\bar{\nabla}^2 \bar{\phi} \rightarrow e^{-2n\pi i/4} \bar{\nabla}^2 e^{-n\pi i/4} \bar{\phi} = e^{-3n\pi i/4} \bar{\nabla}^2 \bar{\phi}, \quad (30)$$

$$\bar{\nabla}^2 \bar{\varphi} \rightarrow e^{-2n\pi i/4} \bar{\nabla}^2 e^{-5n\pi i/4} \bar{\varphi} = e^{n\pi i/4} \bar{\nabla}^2 \bar{\varphi}. \quad (31)$$

Thus, while $\bar{\nabla}^2 \bar{\phi}$ transforms as φ , $\bar{\nabla}^2 \bar{\varphi}$ transforms as ϕ .

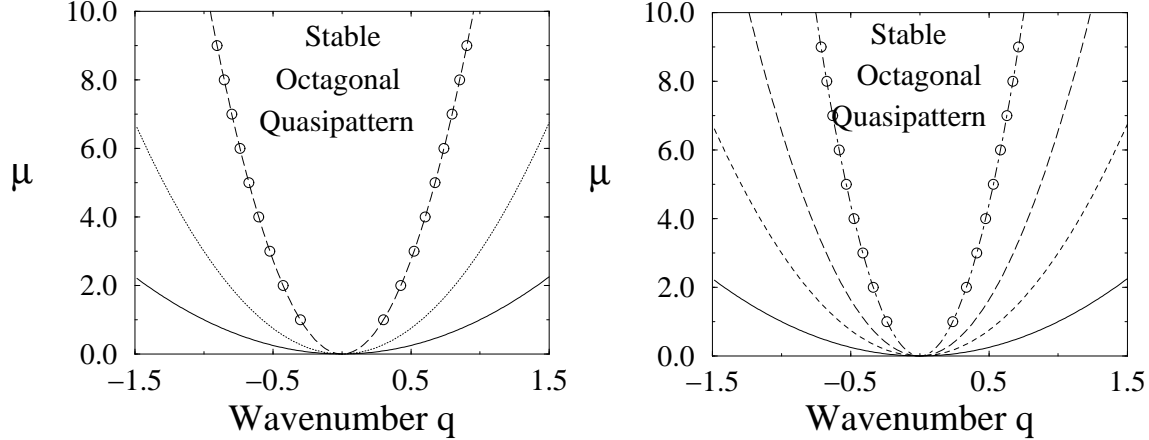


Fig. 3. Stability diagrams for a) $\nu = \gamma = 0.5$, b) $\nu = 0.7$, $\gamma = 0.4$. The dotted, dashed, and dot-dashed lines correspond to $D'_2 = 0$, $D'_5 = 0$ and $D_1 = 0$, respectively. The circles are obtained solving the full dispersion relation associated with Eqs. (15), (16).

In order to calculate the stability boundaries, normal modes must be considered: $\phi = \phi_0 e^{i\mathbf{Q}\cdot\mathbf{x}}$, $\varphi = \varphi_0 e^{i\mathbf{Q}\cdot\mathbf{x}}$. From Eqs. (19)-(22), it can be shown that the stability curves are given by the expression:

$$2D_1 D_2 D_4 D_5 = D_3^2 [(D_1 + D_2)(D_4 + D_5) - 2D_3^2], \quad (32)$$

or, using Eqs. (23)-(27),

$$D_1^2 D'_2 D'_5 = 0. \quad (33)$$

Thus, two eigenvalues become zero when $D_1 = 0$ and the other two when $D'_2 = 0$ and $D'_5 = 0$, respectively. From this, the stability curves are given by:

$$D_1 = 0 \Rightarrow \mu_1 = \frac{3 + \nu + 4\gamma}{1 - \nu} q^2, \quad (34)$$

$$D'_2 = 0 \Rightarrow \mu_2 = 3q^2, \quad (35)$$

$$D'_5 = 0 \Rightarrow \mu_5 = \frac{3 + 3\nu + 2\gamma}{1 + \nu - 2\gamma} q^2. \quad (36)$$

It is interesting to note that the instability corresponding to $D'_2 = 0$ is given by the usual value for the Eckhaus curve. Typical stability diagrams are shown in Fig. 3. When $\nu = \gamma$ the problem is degenerate and $\mu_1 = \mu_5$ (Fig. 3a). Which instability occurs first depends on the values of the coefficients ν and γ . For $\gamma > 0$, $\nu < \gamma$; $\nu + \gamma < 0$, $\gamma < 0$; and $\nu + \gamma > 0$, $\nu > \gamma$ the first instability is that corresponding to D'_5 , D'_2 , and D_1 , respectively. The third case is shown in Fig. 3b. The symbols denote the results of a stability analysis using the full

dispersion relation without the long-wave approximation. They show that the relevant instabilities are long-wave.

In general, the eigenvalues depend on the angle of the perturbation. When $\theta = \arctan(Q_y/Q_x) = n\pi/4$ there is an eigenvalue that is always marginal. (From Eqs. (15), (16) it is easy to see that the growth rate of a perturbation to the phase ϕ_i in a direction perpendicular to $\hat{\mathbf{n}}_i$, is zero). This means that the perturbations perpendicular to each set of rolls evolve on a still slower time scale that is not captured with Eqs. (1). This situation is equivalent to that of the zig-zag instability of rolls or squares [23,24]. In order to resolve this degeneracy we must take Newell-Whitehead-Segel derivative terms in Eqs. (1), using the replacement

$$(\hat{\mathbf{n}}_i \cdot \nabla)^2 \rightarrow [(\hat{\mathbf{n}}_i \cdot \nabla) - i\delta\nabla^2]^2, \quad (37)$$

where δ is a small coefficient, whose size depends on the distance from threshold, $\delta = O(\eta)$.

Assuming that the phase of each of the modes only depends on the direction perpendicular to that mode, it is easy to see that the equations decouple. Introducing a super-slow time, $\partial_T = \epsilon^4 \partial_{T_4}$, and taking q to be small, $q = \epsilon^2 \tilde{q}$, the usual nonlinear phase equation for the zig-zag instability is obtained:

$$\partial_{T_4} \phi_i = 2\tilde{q}\delta(\hat{\tau}_i \cdot \nabla)^2 \phi_i - \delta^2(\hat{\tau}_i \cdot \nabla)^4 \phi_i + 6\delta^2[(\hat{\tau}_i \cdot \nabla)\phi_i]^2(\hat{\tau}_i \cdot \nabla)^2 \phi_i, \quad (38)$$

where $\hat{\tau}_i$ is the unit vector perpendicular to $\hat{\mathbf{n}}_i$. When $\tilde{q} < 0$ the pattern is unstable. As the coefficient in front of the cubic term is positive, the instability is supercritical. In order to confirm this we have performed numerical simulations of Eqs. (1) using a fourth-order Runge-Kutta method with an integrating factor that computes the linear derivative terms exactly in Fourier space. In Fig. 4 the evolution of this zig-zag instability is shown, starting with a perturbation of the quasipattern in the direction perpendicular to $\hat{\mathbf{n}}_1$: $A_1 = Re^{iqx}(1 + 0.1i \cos(4\pi y/L))$, $A_j = Re^{iq\hat{\mathbf{n}}_j \cdot \mathbf{x}}$, $j \neq 1$. As expected, the instability saturates, resulting in a distorted quasipattern.

3 Decagonal Quasipatterns

3.1 Ginzburg-Landau Equations

For the decagonal quasipattern we consider the expansion (cf. Fig. 1b) $\psi = \eta \sum_{n=1}^5 A_n(\mathbf{x}, t) e^{i\mathbf{k}_n \cdot \mathbf{x}} + c.c. + h.o.t..$ The amplitudes $A_i(\mathbf{x}, t) \equiv r_i e^{i\phi_i}$ now satisfy the equations

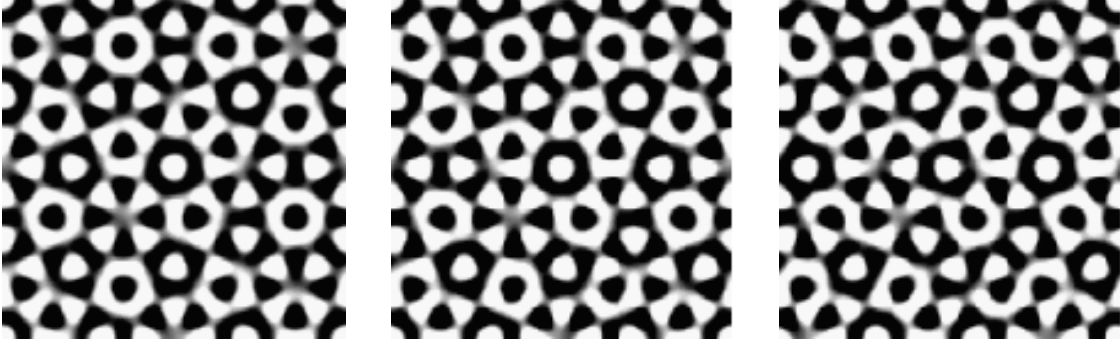


Fig. 4. Reconstruction of the octagonal quasipattern from the amplitudes A_i for the zigzag instability at the times a) $t=0$, b) $t=1000$, and c) $t=3000$. The simulations are done with 64×64 Fourier modes and the values of the coefficients: $\mu = 5$, $\nu = 0.7$, $\gamma = 0.4$, $q = -0.05$, $L = 25$, $k_c = 10k_{min}$ and $\delta = 0.1$.

$$\begin{aligned} \partial_t A_i = & \mu A_i + (\hat{\mathbf{n}}_i \cdot \tilde{\nabla})^2 A_i - A_i[|A_i|^2 + \nu(|A_{i+1}|^2 + |A_{i+4}|^2) \\ & + \gamma(|A_{i+2}|^2 + |A_{i+3}|^2)] + \alpha \overline{A_{i+1} A_{i+2} A_{i+3} A_{i+4}}, \end{aligned} \quad (39)$$

where μ is the control parameter and ν and γ measure the interaction between modes subtending an angle of $2\pi/5$ and $4\pi/5$, respectively. The indices are repeated cyclically with period 5. Although the quartic term is higher order than the others, we have included it in Eq. (39) to account for the resonant interaction among the five wavevectors, $\sum_{j=1}^5 \hat{\mathbf{k}}_j = 0$ (see Fig. 1b). Without this term there would be a spurious one-parameter class of solutions, parameterized by the global phase, $\Phi = \sum_{j=1}^5 \phi_j$, all with the same energy. The resonance term lifts this degeneracy by rendering the global phase (slightly) damped.

The Lyapunov functional for the dodecagonal case is given by

$$\begin{aligned} \mathcal{F} = & \int \int dx dy \sum_{i=1}^5 \left[-\mu |A_i|^2 + |(\hat{\mathbf{n}}_i \cdot \tilde{\nabla})^2 A_i|^2 + \frac{1}{2} |A_i|^4 + \nu |A_i|^2 |A_{i+1}|^2 \right. \\ & \left. + \gamma |A_i|^2 |A_{i+2}|^2 \right] - \alpha (A_1 A_2 A_3 A_4 A_5 + c.c.). \end{aligned} \quad (40)$$

Writing again $A_j = a_j e^{i\phi_j}$, we now have:

$$\begin{aligned} \partial_t a_i = & \mu a_i - a_i [a_i^2 + \nu(a_{i+1}^2 + a_{i+4}^2) + \gamma(a_{i+2}^2 + a_{i+3}^2)] \\ & + \alpha a_{i+1} a_{i+2} a_{i+3} a_{i+4} \cos(\Phi), \end{aligned} \quad (41)$$

$$a_i \partial_t \phi_i = -\alpha a_{i+1} a_{i+2} a_{i+3} a_{i+4} \sin(\Phi), \quad (42)$$

with $\Phi = \sum_{j=1}^5 \phi_j$ the global phase. For a quasiperiodic solution $a_1 = \dots = a_5 = R$ and Eq. (42) becomes:

$$\partial_t \Phi = -5\alpha R^3 \sin(\Phi). \quad (43)$$

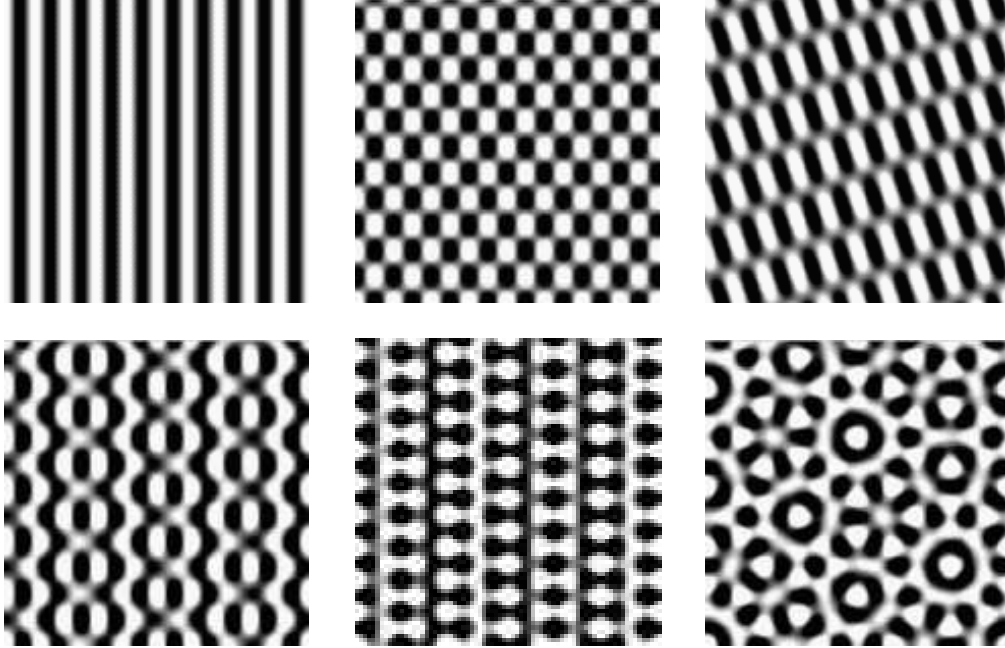


Fig. 5. Decagonal Case. Different types of solutions of Eqs. (39). a) Rolls, b) rectangles R_1 , c) rectangles R_2 , d) and e) 1D quasipatterns H_1 and H_2 , and f) decagonal quasipattern.

There are two solutions, one stable ($\Phi = 0$), the other unstable ($\Phi = \pi$). We will consider the former one.

Because the resonant term involving α is quartic, it cannot appear in systems with the reflection symmetry $A_i \rightarrow -A_i$ which arises, for instance, in Boussinesq convection or in Faraday waves with one-frequency forcing. In that case ($\alpha = 0$) Φ is arbitrary to the order considered in Eq. (39) and, for $\Phi \neq 0, \pi$, solutions with pentagonal rather than decagonal symmetry can bifurcate from the trivial state. The situation is analogous to that of the triangle solutions in the case of hexagonal symmetry [25]. The global phase gets fixed by the higher-order resonance term $\bar{A}_i |A_{i+1}|^2 |A_{i+2}|^2 |A_{i+3}|^2 |A_{i+4}|^2$, which leads to $\partial_t \Phi \sim \sin(2\Phi)$, implying $\Phi = n\pi/2$ for the regular pentagonal solution. We will not consider these solutions in the following and take $\phi_1 = \dots = \phi_5 = 0$.

There are six different kinds of simple solutions (see Fig. 5): rolls, two types of rectangles, two types of one-dimensional quasipatterns and the decagonal quasipattern. They are given by:

- (1) Rolls: $a_2 = \dots = a_5 = 0$ and $a_1 = \sqrt{\mu}$, $F_R = -\mu^2/2$.
- (2) Rectangles (R_1): $a_1 = a_2 = a_5 = 0$ and $a_3 = a_4 = \sqrt{\mu/(\nu + 1)}$, $F_{R_1} = -\mu^2/(\nu + 1)$.
- (3) Rectangles (R_2): $a_2 = a_3 = a_5 = 0$ and $a_1 = a_4 = \sqrt{\mu/(\gamma + 1)}$, $F_{R_2} =$

$$-\mu^2/(\gamma + 1).$$

(4) One-dimensional quasipatterns (H_1): $a_2 = a_5 = 0$ and

$$a_1 = \sqrt{\frac{\mu(1 + \nu - 2\gamma)}{1 + \nu - 2\gamma^2}}, \quad a_3 = a_4 = \sqrt{\frac{\mu(1 - \gamma)}{1 + \nu - 2\gamma^2}}, \quad (44)$$

$$F_{H_1} = -\frac{\mu^2}{2} \frac{\nu + 3 - 4\gamma}{\nu - 2\gamma^2 + 1}. \quad (45)$$

They exist provided $(1 - \gamma)(1 + \nu - 2\gamma) > 0$.

(5) One-dimensional quasipatterns (H_2): $a_3 = a_4 = 0$ and

$$a_1 = \sqrt{\frac{\mu(1 + \gamma - 2\nu)}{1 + \gamma - 2\nu^2}}, \quad a_2 = a_5 = \sqrt{\frac{\mu(1 - \nu)}{1 + \gamma - 2\nu^2}}, \quad (46)$$

$$F_{H_2} = -\frac{\mu^2}{2} \frac{3 + \gamma - 4\nu}{1 + \gamma - 2\nu^2}. \quad (47)$$

They exist provided $(1 - \nu)(1 + \gamma - 2\nu) > 0$. Both, H_1 and H_2 are quasiperiodic in one dimension and periodic in the other.

(6) Quasipattern: $a_1 = \dots = a_5 = R$, with R satisfying

$$0 = \mu - (1 + 2\nu + 2\gamma)R^2 + \alpha R^3. \quad (48)$$

The analytic solution is quite complicated. For $\alpha = 0$ it simplifies to

$$R = \sqrt{\frac{\mu}{1 + 2\nu + 2\gamma}} \Rightarrow F_Q = -\frac{5}{2} \frac{\mu^2}{1 + 2\nu + 2\gamma}. \quad (49)$$

(7) In addition, when $\alpha = 0$ there is another solution, with $a_5 = 0$ and

$$a_1 = a_4 = \sqrt{\frac{\mu(1 - \nu)}{1 + \gamma + \nu + \gamma\nu - \nu^2 - \gamma^2}}, \quad (50)$$

$$a_2 = a_3 = \sqrt{\frac{\mu(1 - \gamma)}{1 + \gamma + \nu + \gamma\nu - \nu^2 - \gamma^2}}. \quad (51)$$

It is also quasiperiodic in the two spatial dimensions and exists if $(1 - \nu)(1 - \gamma) > 0$.

The conditions for linear stability are:

(1) Rolls: $\nu > 1, \gamma > 1$.

(2) Rectangles R_1 : $-1 < \nu < 1, \gamma > 1$.

(3) Rectangles R_2 : $\nu > 1, -1 < \gamma < 1$.

(4) 1D quasipattern H_1 :

$$2\gamma - 1 < \nu < 1, \quad (52)$$

$$1 - \nu \frac{1 + \sqrt{5}}{2} - \gamma \frac{1 - \sqrt{5}}{2} < 0 \quad (53)$$

(5) 1D quasipattern H_2 :

$$2\nu - 1 < \gamma < 1, \quad (54)$$

$$1 - \nu \frac{1 - \sqrt{5}}{2} - \gamma \frac{1 + \sqrt{5}}{2} < 0 \quad (55)$$

(6) The quasiperiodic solution given by Eqs. (50), (51) is always unstable.

(7) Decagonal quasipattern:

$$1 - \nu \frac{1 + \sqrt{5}}{2} - \gamma \frac{1 - \sqrt{5}}{2} + R\alpha > 0, \quad (56)$$

$$1 - \nu \frac{1 - \sqrt{5}}{2} - \gamma \frac{1 + \sqrt{5}}{2} + R\alpha > 0, \quad (57)$$

$$2(1 + 2\nu + 2\gamma) - 3\alpha R > 0. \quad (58)$$

When (58) is violated the quasipattern undergoes a saddle-node bifurcation that generates an unstable branch with larger amplitude (see Fig. 6). For these amplitudes the quartic term is of the same order as the other terms in Eq. (39), which is inconsistent with the amplitude expansion. We restrict ourselves therefore to the range $3\alpha R \ll 2(1 + 2\nu + 2\gamma)$.

For $R = 0$ Eqs. (56,57) are complementary to the stability conditions (53) and (55) for the one-dimensional quasipatterns. Thus, at onset one of the one-dimensional quasipatterns can be stable while the two-dimensional quasipattern is unstable (or vice versa). For $\alpha > 0$, the two-dimensional quasipattern can gain stability with increasing μ while the one-dimensional quasipattern is still stable. This bistability is expected to persist even if higher-order terms were included in the Ginzburg-Landau equations (39), since they would contribute only terms of the order R^2 to the stability conditions. For a small range of parameters ν and γ the stabilization of the two-dimensional quasipattern can occur for amplitudes for which these higher-order terms would still be negligible.

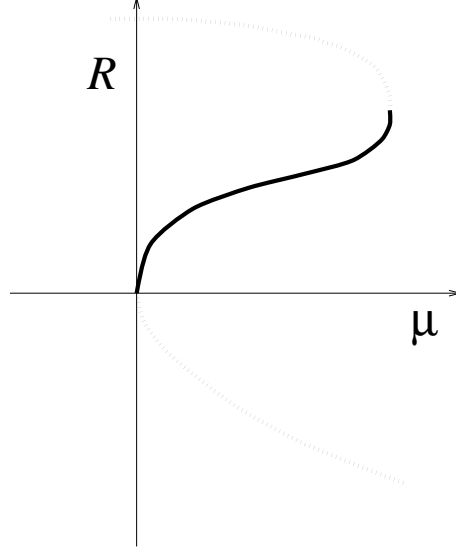


Fig. 6. Sketch of the bifurcation diagram for the decagonal quasipattern, as given by Eq. (48) (solid and dotted lines representing stable and unstable branches, respectively). The saddle-node bifurcation occurs at amplitudes for which (39) is not valid any more.

3.2 Longwave analysis

Proceeding as in the case of the octagonal quasipattern we obtain for the linearized perturbation equations

$$\partial_t r_i = -2qR(\hat{\mathbf{n}}_i \cdot \tilde{\nabla})\phi_i + (\hat{\mathbf{n}}_i \cdot \tilde{\nabla})^2 r_i + R^3 \alpha \left(\sum_{j=1}^5 r_j - 2r_i \right) \quad (59)$$

$$\begin{aligned} & -2R^2 r_i - 2\nu R^2 (r_{i+1} + r_{i-1}) - 2\gamma R^2 (r_{i+2} + r_{i-2}), \\ \partial_t \phi_i &= (\hat{\mathbf{n}}_i \cdot \tilde{\nabla})^2 \phi_i + \frac{2q}{R} (\hat{\mathbf{n}}_i \cdot \tilde{\nabla}) r_i - \alpha R^3 \sum_{j=1}^5 \phi_j, \end{aligned} \quad (60)$$

with R satisfying

$$0 = (\mu - q^2) - (1 + 2\nu + 2\gamma)R^2 + \alpha R^3. \quad (61)$$

For the amplitude perturbations there are three eigenvalues. One eigenvalue, $\sigma_R = R^2(3\alpha R - 2 - 4\nu - 4\gamma)$, corresponds to a one-dimensional eigenspace spanned by

$$v_H^T = \frac{1}{\sqrt{5}} [r_1 = 1, r_2 = 1, r_3 = 1, r_4 = 1, r_5 = 1]. \quad (62)$$

The other two eigenvalues are given by $\sigma_{T2,3} = R^2(-2 - 2\alpha R + \nu(1 \pm \sqrt{5}) + \gamma(1 \mp \sqrt{5}))$ and each corresponds to two two-dimensional eigenspaces. Four orthonormal vectors spanning these spaces are

$$v_{T_1}^T = \frac{1}{\sqrt{5 + \sqrt{5}}} \left[-(1 + \sqrt{5})/2, (1 + \sqrt{5})/2, -1, 0, 1 \right], \quad (63)$$

$$v_{T_3}^T = \sqrt{\frac{1}{40}} \left[-(1 - \sqrt{5}), -(1 - \sqrt{5}), -(1 + \sqrt{5}), 4, -(1 + \sqrt{5}) \right], \quad (64)$$

corresponding to σ_{T_2} and

$$v_{T_2}^T = \frac{1}{\sqrt{5 - \sqrt{5}}} \left[-1, (1 - \sqrt{5})/2, -(1 - \sqrt{5})/2, 1, 0 \right], \quad (65)$$

$$v_{T_4}^T = \sqrt{\frac{1}{40}} \left[-(1 - \sqrt{5}), -(1 + \sqrt{5}), -(1 + \sqrt{5}), -(1 - \sqrt{5}), 4 \right], \quad (66)$$

to σ_{T_3} .

The global phase is a stable mode with a one-dimensional subspace spanned by $u_{\Phi}^T = [\phi_1 = 1, \dots, \phi_5 = 1]/\sqrt{5}$. As with the octagonal quasipattern, there are four marginal phase modes. The two corresponding to translations in space can be written as

$$u_{\phi_x}^T = \sqrt{\frac{2}{5}} \left[1, \cos(2\pi/5), \cos(4\pi/5), \cos(6\pi/5), \cos(8\pi/5) \right], \quad (67)$$

$$u_{\phi_y}^T = \sqrt{\frac{2}{5}} \left[0, \sin(2\pi/5), \sin(4\pi/5), \sin(6\pi/5), \sin(8\pi/5) \right]. \quad (68)$$

The two phason modes can be written as

$$u_{\varphi_1}^T = \sqrt{\frac{2}{5}} \left[1, \cos(6\pi/5), \cos(12\pi/5), \cos(18\pi/5), \cos(24\pi/5) \right], \quad (69)$$

$$u_{\varphi_2}^T = \sqrt{\frac{2}{5}} \left[0, \sin(6\pi/5), \sin(12\pi/5), \sin(18\pi/5), \sin(24\pi/5) \right]. \quad (70)$$

Under rotations the phason mode $\tilde{\varphi} = (\varphi_1, \varphi_2)$ changes with twice the rotation angle.

The expansion of the perturbations includes now the global phase,

$$r_i(\mathbf{x}, t) = \epsilon \sum_{j=1}^4 \hat{r}_j^i(\epsilon^{1/2}\mathbf{x}, \epsilon t) v_{\hat{r}_j}^i \quad (71)$$

$$\begin{aligned} \phi_i(\mathbf{x}, t) = \epsilon^{1/2} & [\phi_x(\epsilon^{1/2}\mathbf{x}, \epsilon t) u_{\phi_x}^i + \phi_y(\epsilon^{1/2}\mathbf{x}, \epsilon t) u_{\phi_y}^i \\ & + \varphi_1(\epsilon^{1/2}\mathbf{x}, \epsilon t) u_{\varphi_1}^i + \varphi_2(\epsilon^{1/2}\mathbf{x}, \epsilon t) u_{\varphi_2}^i] + \epsilon \Phi(\epsilon^{1/2}\mathbf{x}, \epsilon t) u_{\Phi}^i, \end{aligned} \quad (72)$$

and the longwave equations can be written as:

$$\partial_t \phi_x = D_1 \nabla^2 \phi_x + D_2 \partial_x (\nabla \cdot \vec{\phi}) + D_3 (\partial_{x^2}^2 \varphi_1 + 2\partial_{xy}^2 \varphi_2 - \partial_{y^2}^2 \varphi_1), \quad (73)$$

$$\partial_t \phi_y = D_1 \nabla^2 \phi_y + D_2 \partial_y (\nabla \cdot \vec{\phi}) + D_3 (\partial_{x^2}^2 \varphi_1 - 2\partial_{xy}^2 \varphi_1 - \partial_{y^2}^2 \varphi_2), \quad (74)$$

$$\partial_t \varphi_1 = D_4 \nabla^2 \varphi_1 + D_3 (\partial_{x^2}^2 \phi_x - 2\partial_{xy}^2 \phi_y - \partial_{y^2}^2 \phi_x), \quad (75)$$

$$\partial_t \varphi_2 = D_4 \nabla^2 \varphi_2 + D_3 (\partial_{x^2}^2 \phi_y + 2\partial_{xy}^2 \phi_x - \partial_{y^2}^2 \phi_y). \quad (76)$$

The values of the coefficients are given by

$$D_1 = \frac{1}{4} - \frac{q^2}{u_1}, \quad (77)$$

$$D_2 = \frac{1}{2} - \frac{2q^2}{v}, \quad (78)$$

$$D_3 = D_1, \quad (79)$$

$$D_4 = \frac{1}{2} - \frac{q^2}{u_1} - \frac{q^2}{u_2} = D_1 + \tilde{D}_4, \quad \text{with } \tilde{D}_4 = \frac{1}{4} - \frac{q^2}{u_2}, \quad (80)$$

with $u_1 = R^2(2(R\alpha + 1) - \nu(1 + \sqrt{5}) - \gamma(1 - \sqrt{5}))$, $u_2 = R^2(2(R\alpha + 1) - \nu(1 - \sqrt{5}) - \gamma(1 + \sqrt{5}))$, $v = R^2(2(1 + 2\nu + 2\gamma) - 3R\alpha)$, and R a solution of Eq. (61).

In complex form ($\phi = \phi_x + i\phi_y$, $\varphi = \varphi_1 + i\varphi_2$, $\nabla = \partial_x + i\partial_y$) the phase equations read

$$\partial_t \phi = D_1 |\nabla|^2 \phi + \frac{1}{2} D_2 \nabla (\overline{\nabla} \phi + \nabla \overline{\phi}) + D_3 e^{i\alpha} \overline{\nabla}^2 \overline{\varphi}, \quad (81)$$

$$\partial_t \varphi = D_4 |\nabla|^2 \varphi + D_3 e^{i\alpha} \overline{\nabla}^2 \overline{\phi}. \quad (82)$$

Again, the angle α depends on the relative orientation between the phonon and phason modes. For the basis chosen, $\alpha = 0$.

Considering normal modes $\phi = \phi_0 e^{i\mathbf{Q}\cdot\mathbf{x}}$, $\varphi = \varphi_0 e^{i\mathbf{Q}\cdot\mathbf{x}}$, the eigenvalues now become:

$$\sigma_{1,2} = -\frac{1}{2} \left[D_1 + D_4 \pm \sqrt{(D_1 - D_4)^2 + 4D_3^2} \right] Q^2, \quad (83)$$

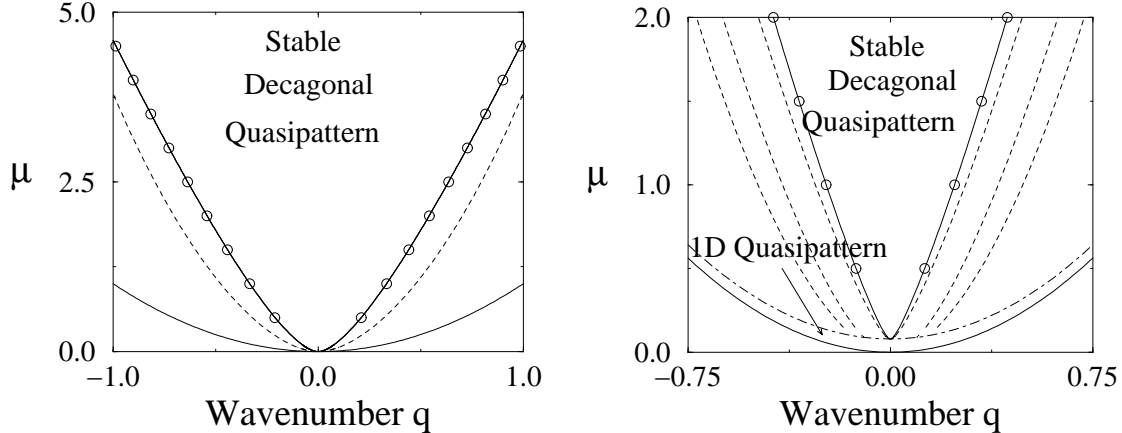


Fig. 7. Stability diagrams for $\alpha = 1$ and a) $\nu = \gamma = 0.7$, b) $\nu = 0.5$, $\gamma = 0.9$. The dash-dotted line represents the line at which the 2-d quasipattern becomes stable. Below this line, the 1-d quasipattern H_2 is the only stable solution.

$$\sigma_{3,4} = -\frac{1}{2} \left[D_1 + D_2 + D_4 \pm \sqrt{(D_1 + D_2 - D_4)^2 + 4D_3^2} \right] Q^2. \quad (84)$$

Typical stability diagrams are shown in Fig. 7. When $\nu = \gamma$ the eigenvalues become degenerate ($D_4 = 2D_1$ and three eigenvalues go through zero at the curve $u_1 = u_2 = 4q^2$.) In Fig.7b the one-dimensional quasipattern persists amplitude-stable beyond the dashed-dotted lines (cf.(55)). We have not investigated its stability with respect to sideband perturbations.

4 Dodecagonal Quasipatterns

4.1 Ginzburg-Landau Equations

Dodecagonal quasipatterns can be thought of as a combination of two rotated hexagon patterns. The amplitudes $A_i(\mathbf{x}, t)$ corresponding to the modes indicated in Fig. 1c satisfy the equations:

$$\begin{aligned} \partial_t A_i = & \mu A_i + (\hat{\mathbf{n}}_i \cdot \tilde{\nabla})^2 A_i + \alpha \overline{A_{i+2} A_{i+4}} - A_i [|A_i|^2 + \nu (|A_{i+2}|^2 + |A_{i+4}|^2) \\ & + \gamma (|A_{i-1}|^2 + |A_{i-3}|^2) + 2\beta |A_{i+1}|^2], \quad i = 1, 3, 5, \end{aligned} \quad (85)$$

$$\begin{aligned} \partial_t A_i = & \mu A_i + (\hat{\mathbf{n}}_i \cdot \tilde{\nabla})^2 A_i + \alpha \overline{A_{i+2} A_{i+4}} - A_i [|A_i|^2 + \nu (|A_{i+2}|^2 + |A_{i+4}|^2) \\ & + \gamma (|A_{i+1}|^2 + |A_{i+3}|^2) + 2\beta |A_{i-1}|^2], \quad i = 2, 4, 6. \end{aligned} \quad (86)$$

Here the indices are cyclic with period 6, μ is the control parameter and ν , γ and β measure the interaction between modes subtending angles of $2\pi/3$, $\pi/6$ and $\pi/2$, respectively. The two hexagonal sub-lattices imply two resonance

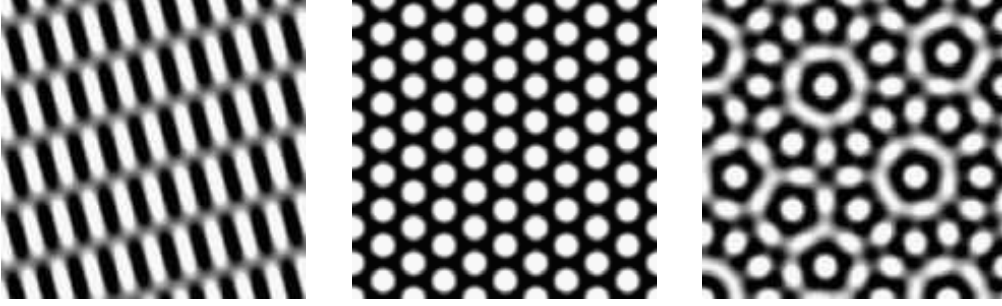


Fig. 8. Dodecagonal Case. Several of the solutions of Eqs. (85), (86). a) Rectangles, b) hexagons, and d) dodecagonal quasipattern.

conditions $\mathbf{k}_1 + \mathbf{k}_3 + \mathbf{k}_5 = 0$ and $\mathbf{k}_2 + \mathbf{k}_4 + \mathbf{k}_6 = 0$. Correspondingly, there are two global phases: $\Phi_1 = \phi_1 + \phi_3 + \phi_5$ and $\Phi_2 = \phi_2 + \phi_4 + \phi_6$.

The Lyapunov functional can be written as:

$$\begin{aligned} \mathcal{F} = \int \int dx dy \sum_{i=1}^6 & \left[-\mu |A_i|^2 + |(\hat{\mathbf{n}}_i \cdot \tilde{\nabla})^2 A_i|^2 + \frac{1}{2} |A_i|^4 + \nu |A_i|^2 |A_{i+2}|^2 \right. \\ & \left. + \frac{\gamma}{2} |A_i|^2 |A_{i+3}|^2 + \frac{\gamma + 2\beta}{2} |A_i|^2 |A_{i+1}|^2 + \frac{(-1)^{i+1}(\gamma - 2\beta)}{2} |A_i|^2 |A_{i-1}|^2 \right] \\ & - \alpha (A_1 A_3 A_5 + A_2 A_4 A_6 + c.c.). \end{aligned} \quad (87)$$

In terms of the magnitudes a_i and phases ϕ_i Eqs. (85,86) can be written as

$$\begin{aligned} \partial_t a_i = \mu a_i + \alpha a_{i+2} a_{i+4} \cos(\Phi) \\ - a_i [a_i^2 + \nu (a_{i+2}^2 + a_{i+4}^2) + \gamma (a_{i\pm 1}^2 + a_{i\pm 3}^2) + 2\beta |a_{i\pm 1}|^2], \end{aligned} \quad (88)$$

$$a_i \partial_t \phi_i = -\alpha a_{i+2} a_{i+4} \sin(\Phi), \quad (89)$$

where $\Phi = \Phi_1$ or $\Phi = \Phi_2$ for i odd and i even, respectively. For hexagonal or dodecagonal patterns in which the non-zero amplitudes are fixed, $a_i = R$, Eq. (89) becomes

$$\partial_t \Phi_{1,2} = -3\alpha R \sin(\Phi_{1,2}). \quad (90)$$

Among the four solutions $\Phi_{1,2} = 0$ and $\Phi_{1,2} = \pi$ only the one with $\Phi_1 = \Phi_2 = 0$ is stable. In the following we assume the amplitudes A_j to be real and take $\phi_1 = \dots = \phi_6 = 0$. Now the simple solutions include rolls, rectangles, squares, hexagons, mixed modes, one-dimensional quasipatterns and the dodecagonal quasipattern (see Fig. 8). They are given by:

- (1) Rolls: $a_2 = \dots = a_6 = 0$ and $a_1 = \sqrt{\mu}$, $F_R = -\mu^2/2$.

(2) Rectangles (R): $a_2 = \dots = a_5 = 0$ and $a_1 = a_6 = \sqrt{\mu/(\gamma + 1)}$, $F_{R_1} = -\mu^2/(\gamma + 1)$.

(3) Squares (S): $a_3 = \dots = a_6 = 0$ and $a_1 = a_2 = \sqrt{\mu/(2\beta + 1)}$, $F_{R_2} = -\mu^2/(2\beta + 1)$.

(4) Hexagons (H): $a_2 = a_4 = a_6 = 0$ and

$$a_1 = a_3 = a_5 = \frac{\alpha \pm \sqrt{\alpha^2 + 4\mu(1 + 2\nu)}}{2(1 + 2\nu)}, \quad (91)$$

$$F_H = -\frac{3}{2}R^2[2\mu - R^2(1 + 2\nu)] - \alpha R^3. \quad (92)$$

(5) Mixed mode, $a_2 = a_4 = a_6 = 0$, $a_1 = a_3 \neq a_5$. It is always unstable.

(6) One-dimensional quasipattern, $a_2 = a_4 = 0$, $a_{1,3,5,6} \neq 0$.

(7) Two-dimensional Quasipattern, $a_1 = \dots = a_6 = R$, with R given by,

$$R = \frac{\alpha \pm \sqrt{\alpha^2 + 4\mu(1 + 2\nu + 2\gamma + 2\beta)}}{2(1 + 2\nu + 2\gamma + 2\beta)}, \quad (93)$$

$$F_Q = -3R^2[2\mu - R^2(1 + 2\nu + 2\gamma + 2\beta)] - 2\alpha R^3. \quad (94)$$

The relative stability of the former solutions is as follows:

(1) Rolls are always unstable at onset. Provided $\nu > 1$, $\beta > 1/2$, and $\gamma > 1$, they become stable at a larger value of μ , given by

$$\mu = \frac{\alpha^2}{(\nu - 1)^2}. \quad (95)$$

(2) Rectangles are unstable at onset and become stable at

$$\mu = \frac{\alpha^2(1 + \gamma)}{(\nu - 1)(\nu + 2\beta - \gamma - 1)}, \quad (96)$$

if $\nu > 1$ and $\nu + 2\beta > \gamma + 1 > 0$.

(3) Squares are also unstable at onset. If $\nu + \gamma > 1 + 2\beta > 0$ they become stable at

$$\mu = \frac{\alpha^2(1 + 2\beta)}{(1 + 2\beta - \nu - \gamma)^2}. \quad (97)$$

(4) Hexagons appear in a saddle-node bifurcation at

$$\mu = -\frac{\alpha^2}{4(1+2\nu)}, \quad (98)$$

but when $2(\gamma + \beta) < -(1 + 2\nu)$ they are always unstable with respect to the dodecagonal quasipattern. If $2(\gamma + \beta) > -(1 + 2\nu)$ they are stable at the saddle-node but can become unstable as a result of a secondary bifurcation. In particular, if $\nu > 1$ they can become unstable to rolls at

$$\mu = \frac{\alpha^2(2 + \nu)}{(\nu - 1)^2}, \quad (99)$$

and, when $1 + 2\nu > 2(\gamma + \beta)$, to the dodecagonal quasipattern for

$$\mu > \frac{2\alpha^2(\gamma + \beta)}{(1 + 2\nu - 2\gamma - 2\beta)^2} \quad (100)$$

(5) Dodecagonal quasipatterns appear in a saddle-node bifurcation at

$$\mu = -\frac{1}{4} \frac{\alpha^2}{(1 + 2\nu + 2\gamma + 2\beta)^2}. \quad (101)$$

When $2|\gamma + \beta| < 1 + 2\nu$, they are unstable at onset with respect to hexagons, but become stable through a secondary bifurcation, at

$$\mu = \frac{\alpha^2}{4} \frac{6\gamma + 6\beta - 2\nu - 1}{(1 + 2\nu - 2\gamma - 2\beta)^2}. \quad (102)$$

Therefore, there is hysteresis between hexagons and the dodecagonal quasipattern. A similar situation is found in the case of superlattices [21].

Besides, if $1 + \gamma < \nu + 2\beta$ or $1 + 2\beta < \gamma + \nu$ the quasipattern becomes again unstable to rectangles or squares, respectively. The values of the control parameter for these transitions are

$$\mu_{rec} = \frac{\alpha^2(3\gamma + \nu + 2)}{(1 + \gamma - \nu - 2\beta)^2}. \quad (103)$$

and

$$\mu_{sq} = \frac{\alpha^2(2 + \gamma + \nu + 4\beta)}{(1 + 2\beta - \gamma - \nu)^2}. \quad (104)$$

4.2 Longwave analysis

The longwave analysis proceeds analogous to that of the previous cases. The linearized perturbation equations are given by:

$$\partial_t r_i = -2qR(\hat{\mathbf{n}}_i \cdot \nabla)\phi_i + (\hat{\mathbf{n}}_i \cdot \nabla)^2 r_i + R\alpha(r_{i+2} + r_{i+4} - r_i) - 2R^2 r_i - 2\nu R^2(r_{i+2} + r_{i+4}) - 2\gamma R^2(r_{i\pm 1} + r_{i\pm 3}) - 4\beta R^2 r_{i\mp 1}, \quad (105)$$

$$\partial_t \phi_i = (\hat{\mathbf{n}}_i \cdot \nabla)^2 \phi_i + \frac{2q}{R}(\hat{\mathbf{n}}_i \cdot \nabla)r_i - \alpha R(\phi_i + \phi_{i+2} + \phi_{i+4}), \quad (106)$$

with

$$R = \frac{\alpha + \sqrt{\alpha^2 + 4(\mu - q^2)(1 + 2\nu + 2\gamma + 2\beta)}}{2(1 + 2\nu + 2\gamma + 2\beta)}. \quad (107)$$

For the amplitude perturbations there are four eigenvalues. Two correspond to one dimensional eigenspaces, $\sigma_{T_1} = -R[2R(1 + 2\nu + 2\gamma + 2\beta) - \alpha]$, with eigenvector $v_{T_1}^T = [1, 1, 1, 1, 1, 1]/\sqrt{6}$ and $\sigma_{T_2} = -R[2R(1 + 2\nu - 2\gamma - 2\beta) - \alpha]$, with $v_{T_2}^T = [-1, 1, -1, 1, -1, 1]/\sqrt{6}$. The other four eigenvalues $\sigma_{T_{3,4}} = -2R[R(1 + \gamma - 2\beta - \nu) + \alpha]$ and $\sigma_{T_{5,6}} = -2R[R(1 + 2\beta - \gamma - \nu) + \alpha]$ are associated with two two-dimensional eigenspaces. Four orthonormal vectors spanning these spaces are:

$$v_{T_3}^T = [-1/2, 1/2, 1/2, -1/2, 0, 0], \quad v_{T_4}^T = [-1/2, 1/2, 0, 0, 1/2, -1/2], \quad (108)$$

corresponding to $\sigma_{T_{3,4}}$ and

$$v_{T_5}^T = [1/2, 1/2, 0, 0, -1/2, -1/2], \quad v_{T_6}^T = [0, 0, 1/2, 1/2, -1/2, -1/2] \quad (109)$$

to $\sigma_{T_{4,5}}$.

The global phases are again stable modes with one-dimensional subspaces spanned by $u_{\Phi_1}^T = [1, 0, 1, 0, 1, 0]/\sqrt{3}$ and $u_{\Phi_2}^T = [0, 1, 0, 1, 0, 1]/\sqrt{3}$. There are four marginal modes. The two phase modes corresponding to translations in space can be written as

$$u_{\phi_x}^T = [1, 0, -1/2, -\sqrt{3}/2, -1/2, \sqrt{3}/2]/\sqrt{3}, \quad (110)$$

$$u_{\phi_y}^T = [0, 1, \sqrt{3}/2, -1/2, -\sqrt{3}/2, -1/2]/\sqrt{3}. \quad (111)$$

An orthonormal base for the phasons, which corresponds to a relative translation of the two hexagonal lattices, is given by:

$$u_{\varphi_1}^T = [1, 0, -1/2, \sqrt{3}/2, -1/2, -\sqrt{3}/2]/\sqrt{3}, \quad (112)$$

$$u_{\varphi_2}^T = [0, 1, -\sqrt{3}/2, -1/2, \sqrt{3}/2, -1/2]/\sqrt{3}. \quad (113)$$

As in the case of the octagonal quasipattern, under rotations the phason field $\tilde{\varphi} = (\varphi_1, \varphi_2)$ changes with five times the rotation angle.

An expansion very similar to that in the decagonal case leads to the longwave equations

$$\partial_t \vec{\phi} = D_1 \nabla^2 \vec{\phi} + (D_2 - D_1) \nabla (\nabla \cdot \vec{\phi}), \quad (114)$$

$$\partial_t \varphi_1 = D_3 \nabla^2 \varphi_1 + (D_4 - D_3) \partial_y (\partial_y \varphi_1 + \partial_x \varphi_2), \quad (115)$$

$$\partial_t \varphi_2 = D_3 \nabla^2 \varphi_2 + (D_4 - D_3) \partial_x (\partial_x \varphi_1 + \partial_y \varphi_2), \quad (116)$$

with $\vec{\phi} = (\phi_x, \phi_y)$. Note that to this order the equation for the phonon modes of the dodecagonal pattern is the same as that for an isotropic medium. The values of the coefficients are:

$$D_1 = \frac{1}{4} - \frac{q^2}{u_1}, \quad (117)$$

$$D_2 = \frac{3}{4} - \frac{2q^2}{v_1} - \frac{q^2}{u_1}, \quad (118)$$

$$D_3 = \frac{1}{4} - \frac{q^2}{u_2}, \quad (119)$$

$$D_4 = \frac{3}{4} - \frac{2q^2}{v_2} - \frac{q^2}{u_2}, \quad (120)$$

with $v_1 = -R[\alpha - 2R(2\beta + 2\nu + 2\gamma + 1)]$, $v_2 = -R[\alpha + 2R(2\beta + 2\gamma - 2\nu - 1)]$, $u_1 = 2R[\alpha + R(1 + \gamma - 2\beta - \nu)]$, $u_2 = 2R[\alpha + R(1 + 2\beta - \gamma - \nu)]$ and R given by Eq. (93).

In complex form the longwave equations become:

$$\partial_t \phi = \frac{1}{2} (D_1 + D_2) |\nabla|^2 \phi + \frac{1}{2} (D_2 - D_1) \nabla (\bar{\nabla} \phi + \nabla \bar{\phi}), \quad (121)$$

$$\partial_t \varphi = \frac{1}{2} (D_3 + D_4) |\nabla|^2 \varphi + \frac{1}{2} (D_3 - D_4) \bar{\nabla}^2 \bar{\varphi}. \quad (122)$$

One feature that distinguishes the dodecagonal quasipattern from the octagonal and the decagonal quasipattern is the fact that its longwave dynamics decouple into pure phonon and pure phason modes. Thus, the eigenvalues are simply given by

$$\sigma_1 = -D_1 Q^2, \quad \sigma_2 = -D_2 Q^2, \quad \sigma_3 = -D_3 Q^2, \quad \sigma_4 = -D_4 Q^2, \quad (123)$$

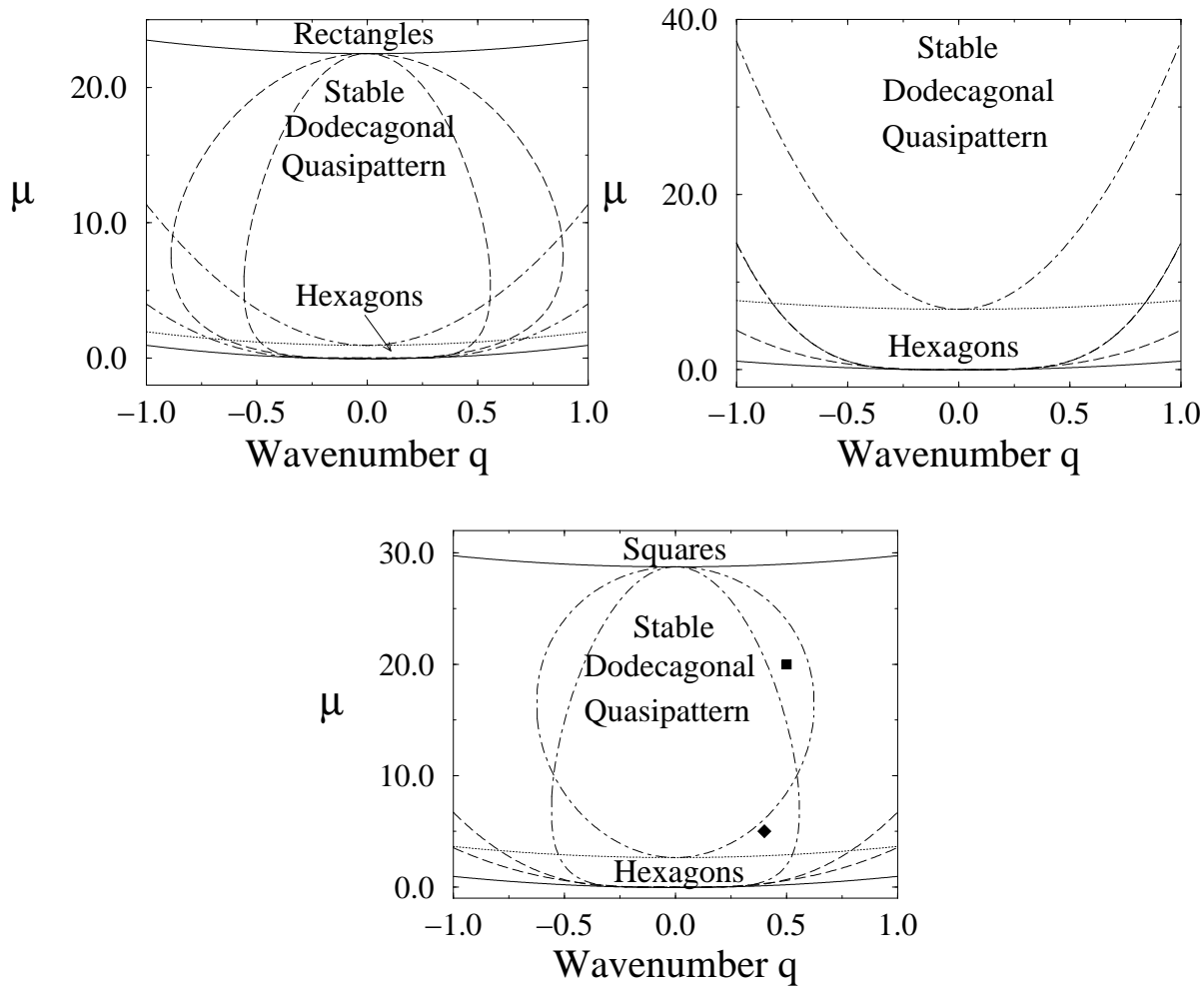


Fig. 9. Stability diagrams for $\alpha = 1$ and a) $\nu = 0.7$, $\gamma = 0.3$ and $\beta = 0.5$, b) $\nu = 0.9$, $\gamma = 0.8$ and $\beta = 0.4$, and c) $\nu = 0.9$, $\gamma = 0.9$ and $\beta = 0.2$. The lower solid line corresponds to the saddle-node bifurcation of the quasipattern. In all the figures the quasipattern is unstable at onset and becomes stable above the dotted line (cf. Eq. (102)). In a) and c) there is a further transition to rectangles and squares, respectively, above the upper solid line. The stable region of the quasipattern is limited by longwave instabilities corresponding to the phonon (long dashed lines) and phason modes (dashed-dotted lines). The diamond and square in c) correspond to the simulations in Figs. 10 and 11, respectively.

and one obtains separate phase and phason instabilities when $D_{1,2}$ or $D_{3,4}$ change sign, respectively. Typical stability diagrams are shown in Fig. 9. The stability limits due to phonon and phason modes are indicated by dashed and dashed-dotted lines, respectively. Over wide ranges of parameters the stable wavenumber band is limited by phason modes.

For the phonon-type modes, the eigenvectors correspond to the usual irrotational and divergence free modes (equivalent to transversal and longitudinal

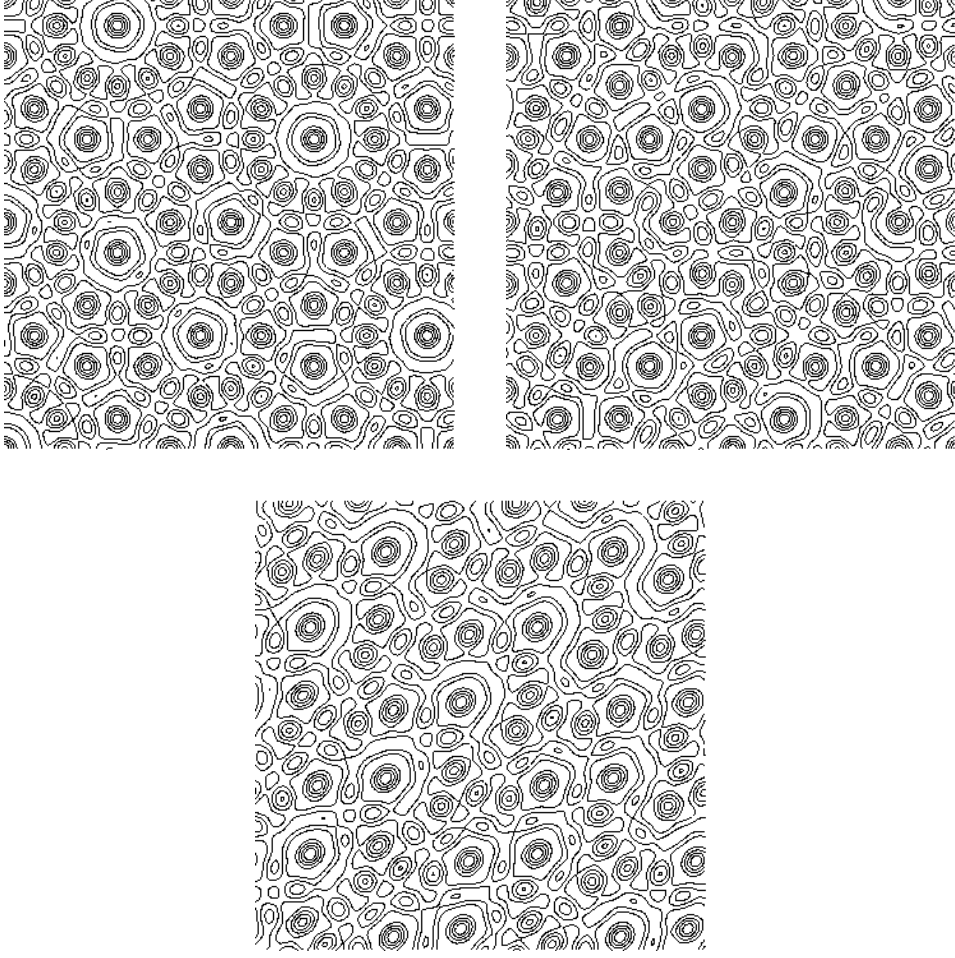


Fig. 10. Instability corresponding to $\sigma_3 > 0$ (diamond in Fig. 9c) for a) $t=0$, b) $t=380$, and c) $t=450$. ($\mu = 5$, $\nu = 0.9$, $\gamma = 0.9$, $\beta = 0.2$, $q = 0.4$, $L = 50$, $k_c = 16k_{min}$).

waves in an elastic medium.) They satisfy:

$$\nabla \cdot \vec{\phi}_l = 0, \quad \nabla \times \vec{\phi}_l = 0. \quad (124)$$

For the phason modes, on the other hand, the eigenvectors are:

$$\tilde{\varphi}^{\sigma_3} = \begin{bmatrix} -Q_x \\ Q_y \end{bmatrix} e^{i\mathbf{Q} \cdot \mathbf{x}}, \quad \tilde{\varphi}^{\sigma_4} = \begin{bmatrix} Q_y \\ Q_x \end{bmatrix} e^{i\mathbf{Q} \cdot \mathbf{x}}. \quad (125)$$

These modes satisfy the equations:

$$\partial_y \varphi_1^{\sigma_3} + \partial_x \varphi_2^{\sigma_3} = 0, \quad \partial_x \varphi_1^{\sigma_4} - \partial_y \varphi_2^{\sigma_4} = 0. \quad (126)$$

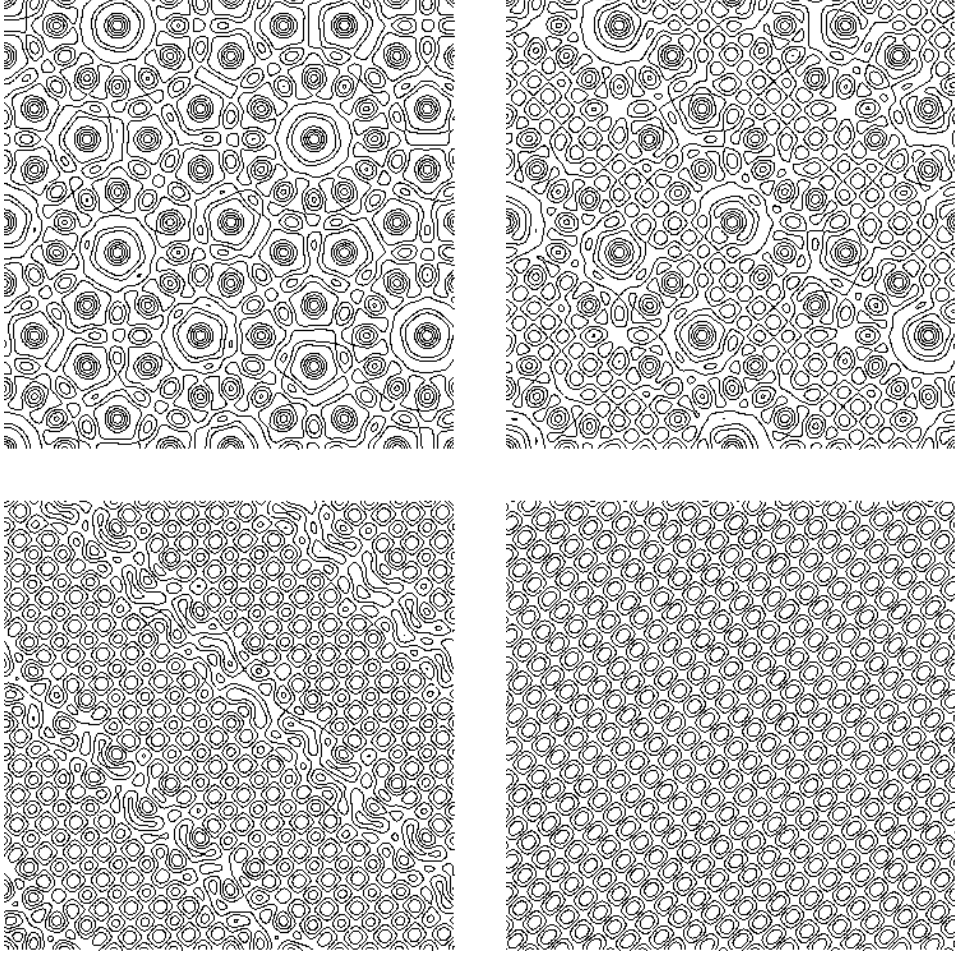


Fig. 11. Instability corresponding to $\sigma_4 > 0$ (square in Fig. 9c) for a) $t=0$, b) $t=440$, c) $t=445$ and d) $t=600$. ($\mu = 20$, $\nu = 0.9$, $\gamma = 0.9$, $\beta = 0.2$, $q = 0.5$, $L = 25$, $k_c = 16k_{min}$).

In order to study the behavior arising from these instabilities we have simulated numerically Eqs. (85), (86). We start with a perfect dodecagonal quasipattern and add a perturbation in the form of $\tilde{\varphi}^{\sigma_3}$ (Fig. 10a) or $\tilde{\varphi}^{\sigma_4}$ (Fig. 11a), with $\mathbf{Q} = (4\pi/L, 4\pi/L)$. Since the perturbation is along the diagonal, the evolution of the system will be quasi one-dimensional. In Fig. 10 we show the evolution of the instability corresponding to $\sigma_3 > 0$. The perturbation grows until it creates line defects at time $t=380$ (Fig. 10b) along which four of the amplitudes vanish and change their wavenumber, demonstrating that the instability is subcritical. In Fig. 10c the final state is shown, after the line defects have gone. It corresponds to a slightly distorted quasipattern.

The instability corresponding to $\sigma_4 > 0$ is also subcritical, generating line defects (Fig. 11b). But for the values of the parameters in the simulation the square pattern minimizes the Lyapunov functional and it nucleates around the line defects. The patches of squares grow (Fig. 11c) until they occupy the whole cell, resulting in a slightly distorted square pattern (Fig. 11d).

5 Defects

The properties of defects in the quasipatterns differ noticeably in the three cases investigated in this paper. Due to the absence of resonance terms in (1) (also to higher orders) the octagonal quasipattern can be considered as made up of four sub-lattices corresponding to the four basic wavevectors. Each of the sub-lattices has its own defects. Thus, taking into account the two possible ‘charges’ of the defects there are 2×4 different defects. They interact strongly with defects of the same sub-lattice *via* the phase. The interaction with the defects in the other sub-lattices is only through the variations in the magnitude and is much weaker. Overall, we expect the dynamics to be quite similar to that of defects in square patterns, which are made of two rather than four sublattices. Topologically, two defects of different sub-lattices could bind to form a vectorial defect (cf. [26]). However, in our simulations we have not observed such kind of defects in the octagonal quasipattern. This seems to be consistent with simulations of the Vector Complex Ginzburg-Landau Equation, where vectorial defects were never observed in the potential limit [27].

For the dodecagonal quasipatterns the Ginzburg-Landau equations (85,86) have (quadratic) resonance terms coupling the three modes in each of the two hexagonal sub-lattices. At the defects therefore two amplitudes in the same sub-lattice must vanish leading to penta-hepta defects very similar to those in the usual hexagonal patterns. However, while in the core of penta-hepta defects of hexagons the pattern corresponds to the roll pattern, it corresponds in the dodecagonal case to the one-dimensional quasipattern. As in the hexagonal case, each penta-hepta defect carries two independent charges corresponding to the two vanishing amplitudes. This leads to a total of $(2 \times 3) \times (2 \times 2) \times 2/2 = 12$ different defects. While in the octagonal case collisions between defects can only annihilate them or leave them unchanged, collisions between penta-hepta defects can change their type. An example of such a collision is given by the process

$$(+, +, 0; 0, 0, 0) + (-, 0, +; 0, 0, 0) \rightarrow (0, +, +; 0, 0, 0). \quad (127)$$

Here $+/-$ in the i^{th} entry stands for a defect with positive/negative charge in the mode A_i while 0 indicates that the corresponding amplitude has no defect. The semi-colon separates the two hexagonal sub-lattices. While there are a number of different such type-changing collisions, a penta-hepta defect in one sub-lattice can never change into one in the other sub-lattice, since there is no resonance term in (85,86) involving modes of both hexagonal sub-lattices. In other words, there is no penta-hepta defect that has one vanishing amplitude in one sub-lattice and one vanishing amplitude in the other sub-lattice.

Penta-hepta defects within the same sub-lattice interact with each other strongly through the phase. The strength of the interaction (attraction *vs.* repulsion) is expected to be related to the sum N of the products of the charges of the individual defects [28],

$$N = \sum_{j=1}^n \delta_j^1 \delta_j^2. \quad (128)$$

Here $\delta_j^{1,2}$ is the topological charge of the first and second defect, respectively, in the mode A_j . For hexagons ($n = 3$) N can only take on the values -2, -1, 1, and 2, since for any defect pair there is always a mode that vanishes in both of them. Thus, within each sublattice all penta-hepta defects interact strongly. Penta-hepta defects of different sub-lattice will interact only weakly (through the magnitude). Considering that collisions do not change defect type across the sublattices, one may expect the ordering dynamics that leads from disordered patterns to ordered quasipatterns to occur in the two sub-lattices essentially independently.

The decagonal case appears to be the most interesting one in terms of the defect dynamics. As in the case of defects in hexagon patterns, the (quartic) resonance term requires that in a defect two amplitudes vanish. In contrast to the hexagonal or dodecagonal case there are, however, two qualitatively different defect types. In one of them the vanishing Fourier modes are rotated by $2\pi/5$ with respect to each other while in the other they are rotated by $2 \times 2\pi/5$. While in the former case the core exhibits the quasipattern H_2 , it is the quasipattern H_1 that appears in the latter case (cf. Fig. 5d,e). Examples of the two cases are shown in Fig. 12a,b. Overall, there are $(2 \times 5) \times (2 \times 4)/2 = 40$ different defects.

The same arguments employed in the hexagonal case [28] suggest that the interaction between defects is richer in the decagonal quasipattern than in hexagons or in the other quasipatterns investigated in the present paper. In hexagonal or dodecagonal patterns two penta-hepta defect pairs always share a mode that vanishes in both pairs and the charge product N given by (128) never vanishes, implying that the defects always interact strongly through the phase. In the decagonal quasipattern, however, the analogously defined N (with $n = 5$) can also take on the value 0, since two pairs of defects need not share a mode with vanishing amplitude. The above argument therefore suggests that in this case the interaction is very weak. We have confirmed this expectation by numerical simulations of the Ginzburg-Landau equations (39). While defect pairs that share a vanishing amplitude ($N \neq 0$) attract or repel each other quite strongly, those with $N = 0$ move so slowly that our preliminary simulations were not able to identify even whether their interaction is attractive or repulsive.

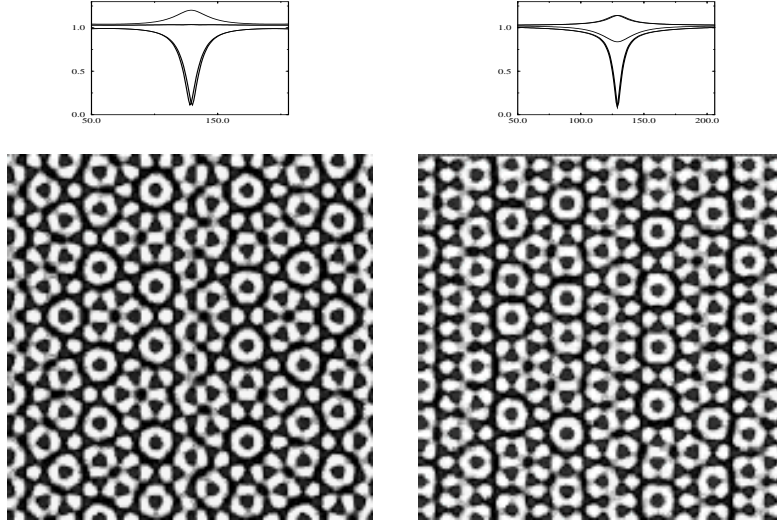


Fig. 12. Decagonal quasipattern with a defect of type a) H_1 and b) H_2 in the center. The top panels show a cross section of the five amplitudes in the x -direction. Two of them vanish at the core of the defect. Of the remaining three, two are equal, as expected from Eqs. (44), (46). In the bottom panels a reconstruction of the physical field ψ is shown. At the core of the defects, the one-dimensional quasipatterns H_1 and H_2 can be observed (compare with Figs. 5d,e).

A separation into weak and strong interaction also arises in the dodecagonal quasipattern. There, however, the division between strong and weak is parallel to the division into the two sublattices. In the decagonal case, however, the resonance term involves all modes and the quasipattern cannot be viewed as the combination of two separate sub-lattices. Correspondingly, a defect of one type can change into a defect of any other type through collisions with suitable other defects. We expect that the exceedingly weak interaction of defect pairs with $N = 0$ may slow down the evolution from disordered or random initial conditions towards an ordered quasipattern.

6 Conclusions

In this paper we have addressed the stability of various types of quasipatterns with respect to long-wave sideband instabilities. For quasipatterns with octagonal, decagonal, and dodecagonal rotational symmetry we have derived from the corresponding Ginzburg-Landau equations long-wave equations for the two phase and the two phason modes. Their stability analysis yields the long-wave stability properties of these patterns.

For the octagonal and the decagonal quasipatterns the phase and the phason modes are coupled and one cannot clearly separate the instabilities in those of the phases and those of the phasons. In these cases our numerical simulations

suggest that the nonlinear behavior arising from the instabilities is the same as that observed in the usual Eckhaus instability. Thus, the instabilities do not saturate within the long-wave equations and lead to the creation of defect pairs which subsequently annihilate each other yielding a stable quasipattern with slightly modified wavevectors. Interestingly, however, in the dodecagonal quasipatterns the phase and phason equations decouple and there are parameter regimes in which the quasipatterns first becomes unstable with respect to phason modes rather than phase modes. The ensuing dynamics appear to be somewhat different than for the usual phase modes. This question has, however, not been pursued in detail in this paper.

The interaction between defects of the decagonal quasipattern can be extremely weak for certain combinations of defects. We expect that this will have a strong influence on the evolution from disordered initial conditions to the regular quasipattern. The investigation of the evolution can most likely not be addressed within the Ginzburg-Landau equations (39) since the ordering dynamics will also entail a spreading of the modes in Fourier space along the critical circle (cf. the dynamics found in hexagon patterns with rotation [29]). This will necessitate the use of suitable equations of the Swift-Hohenberg type.

We gratefully acknowledge discussions with J. Viñals, L. Kramer and M. Silber. This research was supported by NASA (NAG3-2113), the Engineering Research Program of the Office of Basic Energy Sciences at the Department of Energy (DE-FG02-92ER14303) and a grant from NSF (DMS 9804673).

References

- [1] D. Shechtman, I. Blech, D. Gratias, and J. Cahn, *Phys. Rev. Lett.* **53**, 1951 (1984).
- [2] B. Malomed, A. Nepomnyashchy, and M. Tribelsky, *Sov. Phys. JETP* **69**, 388 (1989).
- [3] B. Christiansen, P. Alstrom, and M. Levinsen, *Phys. Rev. Lett.* **68**, 2157 (1992).
- [4] W. Edwards and S. Fauve, *Phys. Rev. E* **47**, 788 (1993).
- [5] E. Pampaloni, P. L. Ramazza, S. Residori, and F. T. Arecchi, *Phys. Rev. Lett.* **74**, 258 (1995).
- [6] A. Golovin, A. Nepomnyashchy, and L. Pismen, *Physica D* **81**, 117 (1995).
- [7] A. Kudrolli, B. Pier, and J. Gollub, *Physica D* **123**, 99 (1998).
- [8] H. Arbell and J. Fineberg, *Phys. Rev. Lett.* (1998).

- [9] H. Arbell and J. Fineberg, Phys. Rev. Lett. **84**, 654 (2000).
- [10] N. D. Mermin and S. M. Troian, Phys. Rev. Lett. **54**, 1524 (1985).
- [11] R. Lifshitz and D. Petrich, Phys. Rev. Lett. **79**, 1261 (1997).
- [12] M. Silber, C. Topaz, and A. Skeldon, Physica D **143**, 205 (2000).
- [13] H. Müller, Phys. Rev. E **49**, 1273 (1994).
- [14] W. Zhang and J. Viñals, Phys. Rev. E **54**, 4283 (1996).
- [15] W. Zhang and J. Viñals, J. Fluid Mech. **336**, 301 (1997).
- [16] P. Chen and J. Viñals, Phys. Rev. E **60**, 559 (1999).
- [17] S. Residori *et al.*, Phys. Rev. Lett. **76**, 1063 (1996).
- [18] E. Pampaloni, S. Residori, S. Soria, and F. Arecchi, Phys. Rev. Lett. **78**, 1042 (1997).
- [19] L. Pismen and B. Rubinstein, Chaos, Solitons & Fractals **10**, 761 (1999).
- [20] B. Dionne, M. Silber, and A. Skeldon, Nonlinearity **10**, 321 (1997).
- [21] M. Silber and M. R. Proctor, Phys. Rev. Lett. **81**, 2450 (1998).
- [22] C. Hu, R. Wang, and D. Ding, Rep. Prog. Phys. **63**, 1 (2000).
- [23] A. Newell and J. Whitehead, J. Fluid Mech. **38**, 279 (1969).
- [24] R. Hoyle, Physica D **67**, 198 (1993).
- [25] M. Golubitsky, J. Swift, and E. Knobloch, Physica D **10**, 249 (1984).
- [26] L. Pismen, Physica D **73**, 244 (1994).
- [27] E. Hernández-García, M. Hoyuelos, P. Colet, and M. S. Miguel, Phys. Rev. Lett. **85**, 744 (2000).
- [28] L. Tsimring, Physica D **89**, 368 (1996).
- [29] B. Echebarria and H. Riecke, Physica D **139**, 97 (2000).